AIP | Applied Physics Letters

Experimental study of an adaptive elastic metamaterial controlled by electric circuits

R. Zhu, Y. Y. Chen, M. V. Barnhart, G. K. Hu, C. T. Sun, and G. L. Huang

Citation: Applied Physics Letters **108**, 011905 (2016); doi: 10.1063/1.4939546
View online: http://dx.doi.org/10.1063/1.4939546
View Table of Contents: http://scitation.aip.org/content/aip/journal/apl/108/1?ver=pdfcov
Published by the AIP Publishing

Articles you may be interested in

Response to "Comment on 'Disentangling longitudinal and shear elastic waves by neo-Hookean soft devices'" [Appl. Phys. Lett. 107, 056101 (2015)]
Appl. Phys. Lett. **107**, 056102 (2015); 10.1063/1.4928393

Steering in-plane shear waves with inertial resonators in platonic crystals
Appl. Phys. Lett. **106**, 223502 (2015); 10.1063/1.4922187

Higher order interaction of elastic waves in weakly nonlinear hollow circular cylinders. II. Physical interpretation and numerical results
J. Appl. Phys. **115**, 214902 (2014); 10.1063/1.4879460

Optimizing the band gap of effective mass negativity in acoustic metamaterials
Appl. Phys. Lett. **101**, 241902 (2012); 10.1063/1.4770370

Theoretical study of shear horizontal wave propagation in periodically layered piezoelectric structure
J. Appl. Phys. **111**, 064906 (2012); 10.1063/1.3694801

This article is copyrighted as indicated in the article. Reuse of AIP content is subject to the terms at: http://scitation.aip.org/termsconditions. Downloaded to IP: 128.206.18.122 On: Tue, 05 Jan 2016 15:55:38

Experimental study of an adaptive elastic metamaterial controlled by electric circuits

R. Zhu,[1,a)] Y. Y. Chen,[1,a)] M. V. Barnhart,[1] G. K. Hu,[2] C. T. Sun,[3] and G. L. Huang[1,b)]
[1]*Department of Mechanical and Aerospace Engineering, University of Missouri, Columbia, Missouri 65211, USA*
[2]*School of Aerospace Engineering, Beijing Institute of Technology, Beijing 100081, China*
[3]*School of Aeronautics and Astronautics, Purdue University, West Lafayette, Indiana 47907, USA*

(Received 24 October 2015; accepted 21 December 2015; published online 5 January 2016)

The ability to control elastic wave propagation at a deep subwavelength scale makes locally resonant elastic metamaterials very relevant. A number of abilities have been demonstrated such as frequency filtering, wave guiding, and negative refraction. Unfortunately, few metamaterials develop into practical devices due to their lack of tunability for specific frequencies. With the help of multi-physics numerical modeling, experimental validation of an adaptive elastic metamaterial integrated with shunted piezoelectric patches has been performed in a deep subwavelength scale. The tunable bandgap capacity, as high as 45%, is physically realized by using both hardening and softening shunted circuits. It is also demonstrated that the effective mass density of the metamaterial can be fully tailored by adjusting parameters of the shunted electric circuits. Finally, to illustrate a practical application, transient wave propagation tests of the adaptive metamaterial subjected to impact loads are conducted to validate their tunable wave mitigation abilities in real-time. © *2016 AIP Publishing LLC*. [http://dx.doi.org/10.1063/1.4939546]

Over the past decade, acoustic/elastic metamaterials (EMMs) have attracted a great deal of attention due to their peculiar dynamic properties, including a negative mass density and stiffness, which are not observed in naturally occurring materials.[1–4] By tailoring the metastructure at the subwavelength scale, acoustic/elastic metamaterials gain the ability to suppress or significantly absorb waves; this opens opportunities for controlling low-frequency wave propagation without the need to scale the structures to unmanageable sizes.[5–10] A metastructure design where the position of the bandgap region could be tailored by choosing or modifying the elastic properties and densities of the constituent materials would be ideal. However, actively controlling the position and size of the bandgap frequency range in real-time is very difficult in practice, if not impossible, for passive metamaterials. One of the most pronounced challenges in acoustic/elastic metamaterial development is the ability to tune their performance without requiring physical microstructural modifications.

The introduction of shunted piezoelectric materials into the metastructure building blocks has the potential to provide a promising method for tuning effective properties where the shunted piezoelectric elements are used as variable stiffness elements. This approach is based on a combination of the inherit properties present in the metamaterial concept with an addition of shunted piezoelectric materials which can be used to alter material properties in real-time. By using shunted piezoelectric materials, an energy exchange between the mechanical and electrical domain can be applied to the metastructure constituent materials. This allows the mechanical properties of the metastructure to be effectively controlled by simple electric circuits. Airoldi and Ruzzene[11] demonstrated that a one-dimensional tunable acoustic metamaterial can be made by using a simple elastic beam fitted with a periodic array of piezoelectric patches connected to resistive-inductive shunted circuits. It was demonstrated that the tunable characteristics of the shunted piezoelectric patches allowed the equivalent mechanical impedance to be tuned so that band gaps could be generated over desired frequency ranges without any modifications to the elastic structures. Two-dimensional periodic arrays of resonant shunted piezoelectric patches have also been used to achieve tunable acoustic metamaterial waveguides.[12–15] The resonance characteristics of the shunts lead to strong attenuation and negative group velocities at frequencies controlled by the electric circuits. Instead of using resonant resistive-inductive shunted circuits, negative capacitance (NC) piezoelectric shunting has also been introduced into the elastic bandgap control of a phononic crystal.[16] Beck *et al.*[17] experimentally demonstrated that a periodic array of piezoelectric patches shunted with NC circuits can control broadband flexural vibrations of a cantilever beam. Celli and Gonella[18] proposed a cellular metamaterial consisting of auxiliary microstructural elements with piezoelectric patches connected to shunted NC circuits. By tuning the circuit parameters, the symmetry of the metamaterial cell can be actively relaxed and therefore, the wave directionality in the metamaterial can be reconfigured. Collet *et al.*[19] developed a numerical approach for modeling and optimizing two-dimensional smart metacomposites with shunted piezoelectric patches. Most recently, Chen *et al.*[20] have implemented the NC piezoelectric shunting into the metastructures to actively tune the locally resonant (LR) frequency by modifying the stiffness of the resonant microstructure and, therefore, controlling the band gap of the active EMM. One advantage of a NC shunted

[a)]R. Zhu and Y. Y. Chen contributed equally to this work.
[b)]Author to whom correspondence should be addressed. Electronic mail: huangg@missouri.edu

 © 2016 AIP Publishing LLC

This article is copyrighted as indicated in the article. Reuse of AIP content is subject to the terms at: http://scitation.aip.org/termsconditions. Downloaded to IP: 128.206.18.122 On: Tue, 05 Jan 2016 15:55:38

circuit is the ability to continuously modify the resonant properties of the metastructures in a broad frequency range. However, there is still a lack of experimental validation of tunable bandgap behavior by considering shunting-piezo-elasto-dynamic effects in the metastructures. Fundamental elucidation of the circuit-feedback electromechanical coupling behavior of the adaptive metastructures is therefore critical for future adaptive metamaterial designs.

In this paper, a design for an adaptive EMM is proposed by integrating the shunted NC piezoelectric patches into the metastructure. The adaptive EMM is then manufactured and its experimental validation for tunable bandgap behavior is performed in a deep subwavelength scale without physical microstructural modifications. Finally, transient wave propagation tests of the adaptive metamaterial subjected to impact loads are conducted to illustrate their tunable wave mitigation abilities in real-time. It can be concluded that the additional degrees of freedom offered by shunted piezoelectric materials can be used to shift the working frequency in the EMM and therefore their adaptive qualities can lead to qualitative improvement for passive metamaterials.

We report a design for a class of adaptive EMMs in which the electric circuits are used to control the subwavelength bandgap behavior in terms of frequency range without requiring microstructural modifications. The unit cell of the LR-based EMM is composed of an acrylic tube with periodically distributed I-type beams and lumped lead masses which are bonded to the central portion of the beam. The adaptive abilities of the EMM are then realized by integrating shunted piezoelectric patches on the opposite surface of the I-type beams. The schematic of the proposed adaptive EMM is shown in Fig. 1(a). The elastic modulus of the shunted piezoelectric patch and the effective bending stiffness of the composite beam can be tailored by adjusting different electric circuit parameters. Therefore, the interior LR frequency of the EMM can be electrically tailored. In the design, two NC circuits, namely, softening and hardening circuits, are implemented to control the shunted piezoelectric patches to decrease and increase the effective bending stiffness of the beam, respectively. The softening circuit consists of a capacitor C_0, a potentiometer R_1, the two resistors R_0 and R_2, and an operational amplifier which can be theoretically operated with the stability condition being negative equivalent capacitances $C_N > C_p$. For a second case, a resistor R_0 in the hardening circuit is replaced by a potentiometer in order to tune and satisfy the stability condition $C_N < C_p$.

To characterize the dynamic properties and provide an underlying physical interpretation of the adaptive metamaterial, a multi-physics effective model should be developed to capture the electro-mechanical coupling effect. However, due to the complex microstructure geometry in the unit cell, it is very difficult to directly derive an analytical model and therefore, a numerical-based multi-physics effective model is utilized to determine the effective properties which are implemented in COMSOL. The effective mass density of the adaptive metamaterial can be calculated based on the macroscopic resultant force and acceleration of the subwavelength metamaterial unit cell which can be obtained by averaging the local quantities on the external boundary of the unit cell in the multi-physics finite element model. The detailed

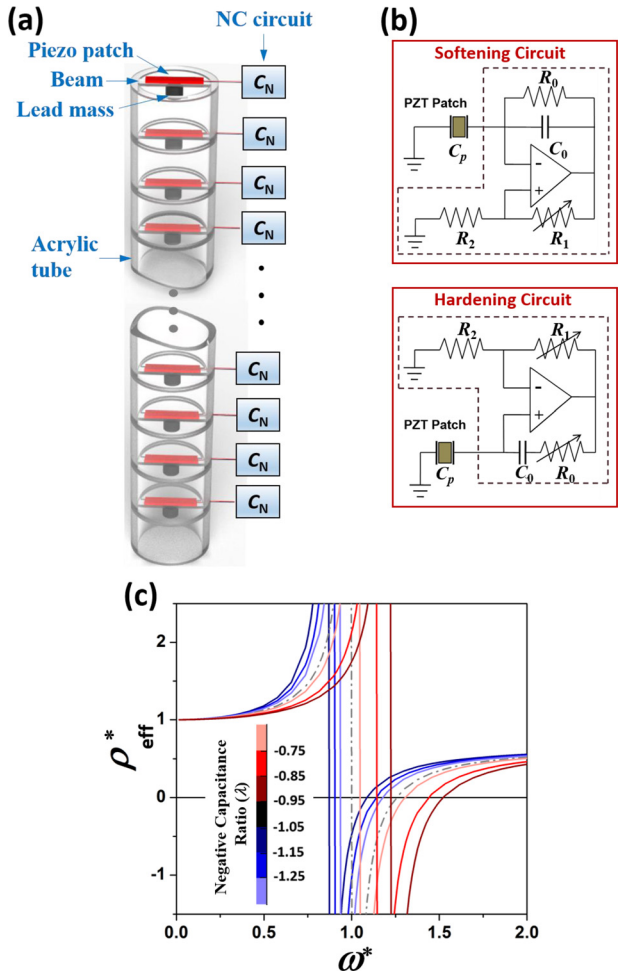

FIG. 1. (a) The schematic of the adaptive EMM. (b) Softening and hardening NC circuits. (c) Effective mass density of the adaptive EMM as a function of both normalized frequency and negative capacitance ratio.

formulation can be found in the supplementary material.[21] Fig. 1(c) shows the numerically calculated tunable effective mass density of the EMM in function of both the normalized frequency ω^* and the negative capacitance ratio λ of the NC circuit, where ρ^*_{eff}, ω^*, and λ are defined as $\rho^*_{eff} = \rho_{eff}/\rho_0$, $\omega^* = \omega/\omega_0$, and $\lambda = C_N/C_p$, respectively. ρ_0 is the static effective density, and ω_0 is the LR angular frequency of the EMM's unit cell with an open circuit where C_p is the capacitance of the piezoelectric patch with the open circuit. It can be found that the frequency range of the negative effective mass density shifts to a lower frequency range when λ approaches to -1 from negative infinity (softening circuits), while it shifts to a higher frequency range when λ approaches to -1 from zero (hardening circuits). Physically, the bandgap of the EMM can be electrically tuned at almost any desired frequency range by adjusting the NC values of the shunted piezoelectric patches without any change to the microstructures geometry. The tunability of the EMM provides a great potential for the design of a gradient-index EMM for applications in elastic wave steering and even elastic wave cloaking. However, in a realistic scenario, system instability due to the NC circuits and the electric damping of the piezoelectric patch can significantly reduce the tunable frequency range of the adaptive EMM, which will be discussed in the experimental validation.

This article is copyrighted as indicated in the article. Reuse of AIP content is subject to the terms at: http://scitation.aip.org/termsconditions. Downloaded to IP: 128.206.18.122 On: Tue, 05 Jan 2016 15:55:38

Dynamic experimental tests are conducted to characterize and validate the dynamic tunability of the adaptive EMM specimen. Fig. 2(a) shows the fabricated adaptive EMM unit cell. The dimensions of the unit cell are given in the supplementary material.[21] Harmonic vibration tests are first performed on the unit cell by using a shaker (LDS V203). The NC circuit (either softening or hardening) is connected to the piezoelectric patch of the unit cell sample and powdered by a DC power supply (Instek SPD-3606). By changing the value of the potentiometer R_1 in the NC circuit, as shown in Fig. 1(b), the value of λ varies in a range close to -1, and the resonant frequency of the unit cell can be tuned electrically. Fig. 2(b) demonstrates the measured voltage signals from the piezoelectric patch when a frequency sweep is conducted. It can be found that the resonant frequency of the adaptive unit cell can be manipulated in a wide frequency range, and the tunability of the resonant frequency, which is defined as $(\omega^*_{max} - \omega^*_{min})$, as high as 45% can be achieved, where ω^*_{max} and ω^*_{min} are the highest and lowest normalized resonant frequencies, respectively. Due to the limitations of the circuits' stability in the experiments, the values of λ should be selected carefully to close to -1 and also satisfy the stability boundaries for both the softening and hardening circuits. Thus, small alterations may either destabilize the system or deteriorate the wave control performance. Fig. 2(c) shows the comparison between the measured results and those obtained from the numerical prediction using the multi-physics numerical model. In the figure, the circuits represent the measured results and the solid curves represent the numerically calculated resonant frequencies of the proposed adaptive unit cell. Very good agreement between the experimental measurement and numerical prediction can be observed, which indicates the feasibility and accuracy of the developed multi-physics numerical model. It should be mentioned that the wavelength in the tunable resonant frequency range is about 30 times larger than the length of the adaptive unit cell.

To quantitatively demonstrate tunable bandgap behavior, an adaptive EMM specimen is formed by assembling nine adaptive unit cells controlled by NC circuits. A tenth cell composed of an empty acrylic tube and circular cap is placed on the top of the EMM for accelerometer installment. In the experimental testing, a white noise excitation signal is first produced by a dynamic analyzer (Bruel & Kjaer PHOTON+) and then amplified by a power amplifier (LDS PA25E) which drives the shaker (LDS V203) to generate an excitation with frequencies from 0 to 1200 Hz. Finally, an accelerometer (Bruel & Kjaer Accelerometer Type 4516) was attached to the top end of the EMM and connected to the dynamic signal analyzer for capturing the transmitted signals. Fig. 3(a) shows the experimentally measured frequency response functions (FRFs) of the adaptive EMM connected to different NC circuits. For comparison, FRFs in the pure acrylic tube and the adaptive EMM with the open circuit are also plotted as dotted and dashed curves, respectively. In the figure, obvious transmission dips can be observed at different frequency ranges for the adaptive EMM connected with different NC circuits, which confirms the tunable wave attenuation ability of the

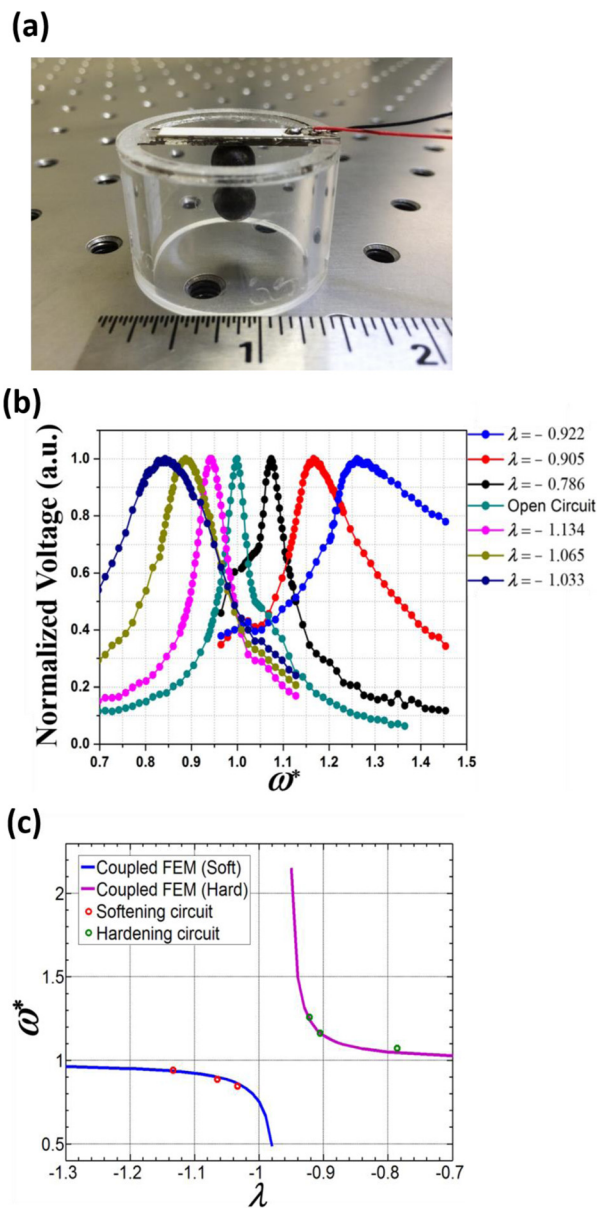

FIG. 2. (a) Photos of the fabricated adaptive unit cell. (b) Measured tunable resonant frequency of the adaptive unit cell when different negative capacitance ratios were applied. (c) Comparison of the resonant frequencies of the unit cell between the experimental testing and numerical simulation.

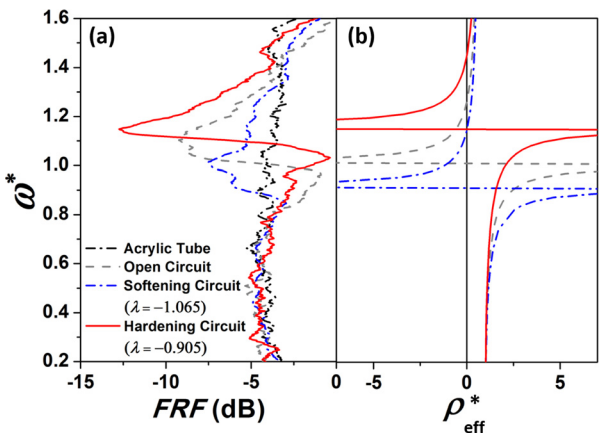

FIG. 3. (a) Experimentally measured frequency response functions of the adaptive EMMs connected with different NC circuits. (b) Numerically calculated effective mass densities with different negative capacitance ratios.

This article is copyrighted as indicated in the article. Reuse of AIP content is subject to the terms at: http://scitation.aip.org/termsconditions. Downloaded to IP: 128.206.18.122 On: Tue, 05 Jan 2016 15:55:38

adaptive EMM sample. Furthermore, the transmission dips can be electronically shifted to different frequency ranges by adjusting circuits (with different λ) without requiring any microstructural modifications. Specifically, the wave attenuation range of the adaptive EMM shifts to the lower frequency range for the EMM with the softening circuits ($\lambda < -1$) and goes to a higher frequency range for the EMM with the hardening circuits ($-1 < \lambda < 0$). To interpret the adaptive wave attenuation mechanism, the tunable effective mass density of the proposed EMM is calculated using the multi-physics numerical model, as shown in Fig. 3(b). It is very interesting to note that the tunable bandgap behavior of the EMM can almost be predicted from the frequency ranges of the tunable negative effective mass density, which indicates that the tunable bandgap behavior is fully controlled by the out-of-phase motions of the EMM and the NC circuits. The minor difference can be attributed to factors from the electric damping and interior loss factor of the piezoelectric patches, which is not considered in the numerical modeling.

Thanks to advantages from the subwavelength-scale size and the high wave attenuation ability, metamaterials were suggested for applications in blast wave mitigation.[22,23] To demonstrate the unique feature of the adaptive EMM, especially in terms of tunable transient wave mitigation, we will further experimentally investigate the transient wave propagation in the adaptive EMM. In the transient wave experiment, a striker, which is made of an aluminum block with a cross section slightly larger than that of the adaptive EMM, is attached to an impact pendulum with adjustable height and impact angle θ to provide impact wave excitation. Consistency of the excitation signals is ensured by precisely controlling the release angle of the impact pendulum, for example, $\theta = 15°$. A steel enclosure disk is glued to the left end of the adaptive EMM specimen to ensure a short incident pulse and mimic the real-world impact excitation. Two miniature piezoelectric sensors (P-6.36 mm-0.33 mm-850, WFB, APC International, LTD.) are bonded before and after the adaptive EMM for measuring the incident and transmitted waves, respectively. A long pure acrylic tube is attached to the right end of the adaptive EMM specimen to separate the reflected wave from the transmitted wave. The entire testing sample is suspended from rigid supports using thin, lightweight strings so as to obtain a free-free boundary condition.

Fig. 4 shows the experimentally measured incident and transmitted wave signals in terms of the electric voltages in both time and frequency domains. In the experiment, three different circuits which are open, hardening ($\lambda = -0.922$), and softening ($\lambda = -1.065$) circuits are used to actively control the wave properties of the adaptive EMMs. From the time domain results, as shown in Figs. 4(a)–4(c), it can be observed that the transmitted pulse is very complex to directly interpret and only an obvious decrease in amplitudes can be observed, which indicates that the incident impact energy has been efficiently attenuated by the adaptive EMM. Moreover, from the frequency-domain results, as shown in Figs. 4(d)–4(f), wave attenuation dips at different frequencies can be clearly observed with different shunted electric circuits. Specifically, it is found that the adaptive EMM with an open circuit has a maximum transmission dip at 680 Hz, while adaptive EMMs with softening ($\lambda = -1.065$) and hardening circuits ($\lambda = -0.922$) have maximum transmission dips at 530 Hz and 1200 Hz, respectively. The difference among the three incident pluses in the frequency domain comes from the reflections of the metamaterial section with different shunted circuit configurations. It should be mentioned that the wave mitigation ability of the adaptive EMM could be significantly increased by adding more EMM unit cells. It can also be conceived that in conjunction with the proper control system, the tunable wave mitigation could

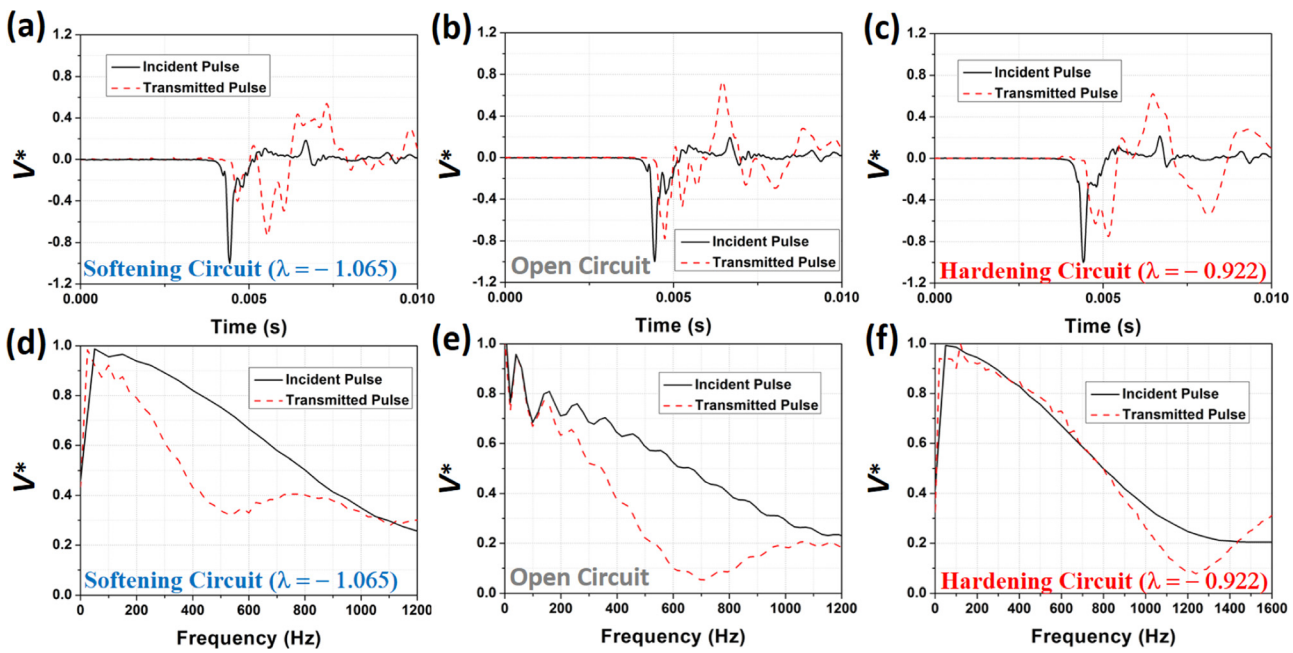

FIG. 4. The time-domain incident and transmitted signals for adaptive EMM with (a) softening circuit ($\lambda = -1.065$), (b) open circuit, and (c) hardening circuit ($\lambda = -0.922$). The frequency-domain incident and transmitted pulses for adaptive metamaterial with (d) softening circuit ($\lambda = -1.065$), (e) open circuit, and (f) hardening circuit ($\lambda = -0.922$).

This article is copyrighted as indicated in the article. Reuse of AIP content is subject to the terms at: http://scitation.aip.org/termsconditions. Downloaded to IP: 128.206.18.122 On: Tue, 05 Jan 2016 15:55:38

be operated in real-time because of the quick response time of the shunted electric circuits.

In this paper, we experimentally investigate the dynamic behavior of an adaptive EMM which is actively controlled by negative capacitance piezoelectric shunting. Based on the multi-physics numerical model developed, the quantitative relationship between the effective mass density of the metamaterial and shunted electric circuits is established. By changing the values of the potentiometer in the negative capacitance circuits, the resonant frequency of the EMM and a tunable bandgap capacity as high as 45% are physically realized by using both shunted hardening and softening circuits. Finally, transient impact wave propagation tests are conducted and the obtained results demonstrate the promising possibilities to dynamically mitigate and filter different wave frequencies in real time.

This work was supported by the Air Force Office of Scientific Research under Grant No. AF 9550-15-1-0061 with Program Manager Dr. Byung-Lip (Les) Lee.

[1]Z. Y. Liu, X. X. Zhang, Y. Mao, Y. Y. Zhu, Z. Yang, C. T. Chan, and P. Sheng, Science **289**, 1734–1736 (2000).
[2]X. N. Liu, G. K. Hu, G. L. Huang, and C. T. Sun, Appl. Phys. Lett. **98**, 251907 (2011).
[3]Y. Wu, Y. Lai, and Z. Q. Zhang, Phys. Rev. Lett. **107**, 105506 (2011).
[4]R. Zhu, X. N. Liu, G. L. Huang, H. H. Huang, and C. T. Sun, Phys. Rev. B **86**, 144307 (2012).
[5]L. Fok, M. Ambati, and X. Zhang, MRS Bull. **33**, 931–934 (2008).
[6]A. Bergamini, T. Delpero, L. D. Simoni, L. D. Lillo, M. Ruzzene, and P. Ermanni, Adv. Mater. **26**, 1343–1347 (2014).
[7]J. Mei, G. Ma, M. Yang, Z. Yang, W. Wen, and P. Sheng, Nat. Commun. **3**, 756 (2012).
[8]Y. Y. Chen, G. L. Huang, X. M. Zhou, G. K. Hu, and C. T. Sun, J. Acoust. Soc. Am. **136**, 969–979 (2014).
[9]R. Zhu, X. N. Liu, G. K. Hu, C. T. Sun, and G. L. Huang, Nat. Commun. **5**, 5510 (2014).
[10]X. Yan, R. Zhu, G. L. Huang, and F. G. Yuan, Appl. Phys. Lett. **103**, 121901 (2013).
[11]L. Airoldi and M. Ruzzene, New J. Phys. **13**, 113010 (2011).
[12]F. Casadei, T. Delpero, A. Bergamini, P. Ermanni, and M. Ruzzene, J. Appl. Phys. **112**, 064902 (2012).
[13]O. Thorp, M. Ruzzene, and A. Baz, Smart Mater. Struct. **10**, 979–989 (2001).
[14]O. Thorp, M. Ruzzene, and A. Baz, Smart Mater. Struct. **14**, 594–604 (2005).
[15]J. F. Deü, W. Larbi, R. Ohayon, and R. Sampaio, J. Vib. Acoust. **136**, 031007 (2014).
[16]S. B. Chen, J. H. Wen, D. L. Yu, G. Wang, and X. S. Wen, Chin. Phys. B **20**, 014301 (2011).
[17]B. S. Beck, K. A. Cunefare, M. Ruzzene, and M. Collet, J. Intell. Mater. Syst. Struct. **22**, 1177–1187 (2011).
[18]P. Celli and S. Gonella, Appl. Phys. Lett. **106**, 091905 (2015).
[19]M. Collet, M. Ouisse, and M. H. Ichchou, J. Intell. Mater. Syst. Struct. **23**, 1661–1677 (2012).
[20]Y. Y. Chen, G. L. Huang, and C. T. Sun, J. Vib. Acoust. **136**, 061008 (2014).
[21]See supplementary material at http://dx.doi.org/10.1063/1.4939546 for the formulation of the multi-physics effective model.
[22]K. T. Tan, H. H. Huang, and C. T. Sun, Int. J. Impact Eng. **64**, 20–29 (2014).
[23]Y. Y. Chen, M. V. Barnhart, J. K. Chen, G. K. Hu, C. T. Sun, and G. L. Huang, Compos. Struct. **136**, 358–371 (2016).

This article is copyrighted as indicated in the article. Reuse of AIP content is subject to the terms at: http://scitation.aip.org/termsconditions. Downloaded to IP: 128.206.18.122 On: Tue, 05 Jan 2016 15:55:38